



Superconducting 70 AMeV cyclotron-injector for a hadron therapy complex

V. Smirnov^{a,*}, S. Vorozhtsov^a, F. Taft^b, T. Matlocha^c

^a Joint Institute for Nuclear Research, Dubna, Russia

^b Amirkabir University of Technology, Tehran, Iran

^c Nuclear Physics Institute of the Czech Academy of Sciences, Rez, Czech Republic

ARTICLE INFO

Keywords:

Cyclotron
Hadron therapy
Superconductivity
Computer simulation
Beam dynamics
Electromagnetic fields

ABSTRACT

An accelerator complex for hadron therapy is under design at the Joint Institute for Nuclear Research (Dubna, Russia). The complex consists of two superconducting cyclotrons. The facility is intended for generating accelerated beams of protons, carbon, and H_2^+ ions. The main cyclotron named K1600 is a separated sector machine, which accelerates carbon ions to the output energy of 400 MeV/u. As an injector, a compact cyclotron K280 is provided for production of proton, carbon, and H_2^+ ion beams with the output energy of 70 MeV/u. The ions are injected into the machine from an ECR ion source. Two extraction methods can be used in the cyclotron. One is based on using an electrostatic deflector and is intended for extracting carbon and H_2^+ ions. The other uses a stripping foil for production of protons from H_2^+ ions. The K280 can also be used as a stand-by facility for medical purposes like treating eye melanoma or for producing radioisotopes. The basic parameters of the cyclotron-injector and detailed investigation of its systems along with the beam dynamics are described.

1. Introduction

An accelerator complex for hadron therapy based on a chain of cyclotrons is under development at the Joint Institute for Nuclear Research (Dubna, Russia) [1]. It is assumed to be a good solution for a wide range of medical applications. The essence of the proposal – following reference [2] – is the usage of two superconducting cyclotrons to facilitate construction and commissioning of the machine.

The complex should have the highest possible efficiency of the beam injection and extraction. The complex is able to produce 70 MeV proton and carbon beams of the energy of 70 MeV/u and 400 MeV/u. The lower-energy beams are suitable for treating eye melanomas and skin cancer [3,4] or producing radiopharmaceuticals. In the radiation therapy, carbon ions of 400 MeV/u possess many advantages over protons. The low-energy beams are accelerated in the compact superconducting cyclotron K280, which is also used as an injector for the superconducting sector cyclotron K1600 to obtain the final energy of 400 MeV/u. The injector-cyclotron for the complex is similar to 250 MeV/u machine for the layout proposed by Schippers et al. [2] and described in [5] but with substantially smaller energy that drastically simplified the design of the machine. The medical facility based on the cyclotron complex has rather moderate overall dimensions (Fig. 1). For proton beam generation in the machine, acceleration of H_2^+ ions with axial injection from the same ECR ion source as for carbon ions can be used. The main parameters of the cyclotron are given in Table 1. The methods and the design concepts of the components used in the paper are mostly described in reference [6].

2. Injection system

It is planned to use a single ECR ion source for injection of $^{12}C^{6+}$ and H_2^+ ion beams. For example, the SUPERNANOGAN ion source sold by PANTECHNIK [8] can produce both $^{12}C^{6+}$ ions with intensity up to 3 eμA and H_2^+ ions with intensity above 1 emA at the maximal extraction voltage of 30 kV [9]. The carbon beam is obtained by mixing CO_2 and He gases. The H_2^+ beam is produced by injecting hydrogen as a single gas at low RF power. The tuning of the source for production of these two beams is totally different, but it is possible to switch from one to the other in few hours. Also, a customer who wants to switch faster can use two SUPERNANOGAN ion source branches with a switching magnet. Alternatively, the Multi-Cusp ion source can be used to produce the H_2^+ beam. The low-energy beam transport line (LEBT) is designed to place the ion source at a distance of 3 m from the cyclotron median plane, where the main magnet fringe field is sufficiently small. After passing through the horizontal section of the LEBT, where the analyzing magnet focuses beam in both transverse directions, the beam enters the axial injection line. The beam intensity in the LEBT can be measured by a Faraday cup, and the beam adjustment can be performed by the electrostatic steerer. There are also three room-temperature solenoids for transverse focusing of the beam in the axial injection line (Fig. 2). Some additional beam shaping and diagnostics elements can be included in the injection system later if recommended by further beam simulations.

* Corresponding author.

E-mail address: vsmirnov@jinr.ru (V. Smirnov).

Table 1
Basic parameters of the cyclotron.

Cyclotron type	Compact, isochronous
Type of accelerated ion	$^{12}\text{C}^{6+}$, H_2^+
Final beam energy	70 MeV/u
Output intensity of the beams: $^{12}\text{C}^{6+}/\text{H}_2^+$ /proton	0.9/300/800 μA
Output $^{12}\text{C}^{6+}$ & H_2^+ & proton beam emittances: (radial/axial)	(23/22) & (21/20) & (30/20) $\pi \cdot \text{mm} \cdot \text{mrad}$
Magnetic structure	3 spiral sectors
Average magnetic field: injection/extraction	2.6 T/2.9 T
Sector angular span	50–38 deg
Spirality	55 deg
Pole radius	920 mm
Hill gap	52 mm
Valley gap	540 mm
Acceleration system	3 spiral cavities
Peak dee voltage	90 kV
Acceleration frequency	60.77 MHz
Acceleration mode	3
External injector	ECRIS
Extraction type: carbon and H_2^+ /proton	Electrostatic deflector/stripping foil
Average extraction radius	870 mm
Dimensions: diameter/height	3000 mm/1400 mm
Total weight	~70 t

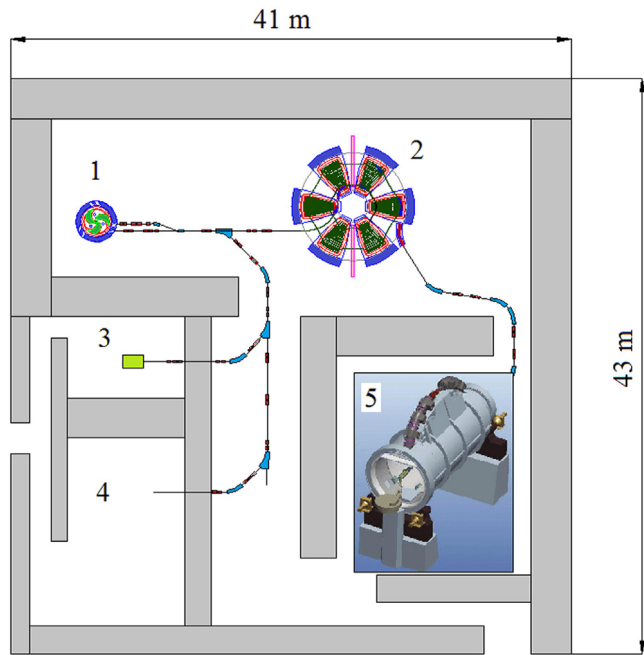


Fig. 1. Medical facility based on a cyclotron complex: 1 — K280 cyclotron, 2 — K1600 cyclotron, 3 — eye melanoma treatment room, 4 — isotope production room, 5 — carbon therapy room, in which superconducting gantry like that in [7] can be used.

In the injection line the beam dynamic simulation was performed starting from the bending magnet exit to the cyclotron center assuming about the same transverse emittances as at the ion source output. Also, the horizontal part of the line should provide an upright shape of these emittances at the dipole exit. According to the available technical description, the transverse emittances of the beam exiting the ion source is about $50 \pi \cdot \text{mm} \cdot \text{mrad}$.

The axial magnetic field produced by the cyclotron magnet in the injection line is rather high, leading to strong over-focusing of the particles that induces a large angular spread in the beam. The effect can be adjusted by the solenoid closest to the main cyclotron magnet having the field direction opposite to the direction of the machine fringe field. Length of solenoids is 200 mm and nominal fields are 500, 1700, and -1000 Gs. The beam matching by the Trace3D code [10] well agrees with the SNOP code results [11,12], having satisfactory

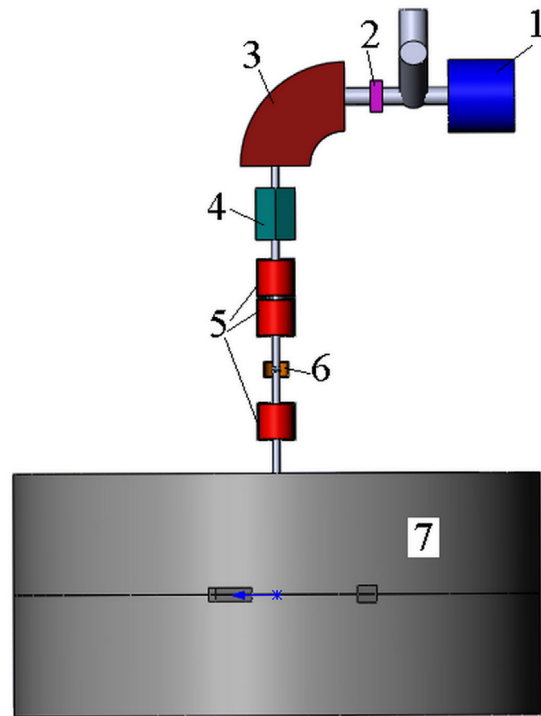


Fig. 2. K280 injection system: 1 — ECRIS, 2 — steerer, 3 — bending magnet, 4 — Faraday cup, 5 — solenoids, 6 — buncher, 7 — cyclotron.

transverse beam envelopes in the line (Fig. 3). The main requirement is to have the beam transversal size at the inflector entrance not more than 3 mm in order to provide acceptable beam transmission through the cyclotron central region.

In the line the sine-wave buncher ensures longitudinal focusing of the injected beam. The buncher has two parallel grids with a 2-mm spacing between the $50 \mu\text{m}$ thick-wires for the field shaping. The buncher transparency for the beam is $\sim 97\%$ with the grid spacing of 5 mm and entrance aperture of 24 mm. The buncher is located at a minimal transverse size of the beam. The distance from the buncher to the cyclotron midplane is 1300 mm, and the RF amplitude is 350 V to have the longitudinal focus of the beam exactly on the cyclotron center. In both regimes of operation – carbon ions and H_2^+ ions – the same buncher voltage can be used.

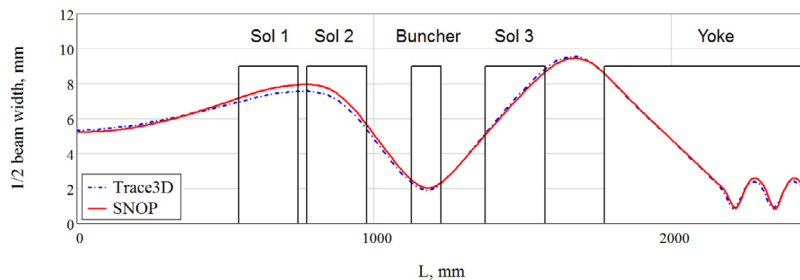


Fig. 3. Beam envelopes (two standard deviations) in the axial part of the injection line.

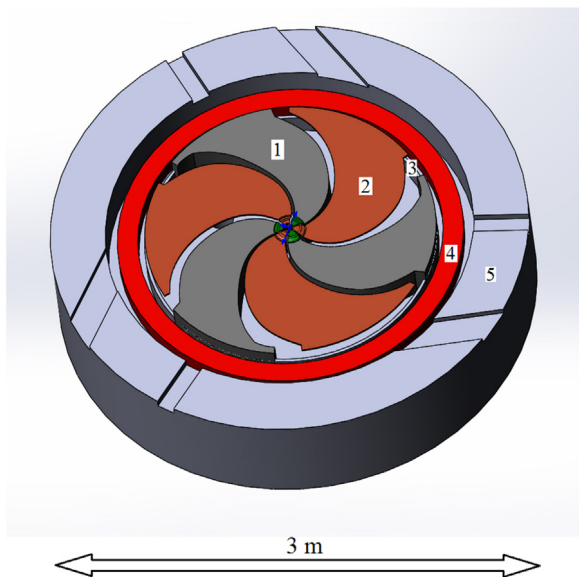


Fig. 4. Magnetic system of the cyclotron: 1 — sector, 2 — dee, 3 — valley shim, 4 — coil, 5 — yoke.

3. Magnetic system

The cyclotron magnetic system has a 3-fold structure (Fig. 4). The selection of the central field of 2.64 T is defined by the requirement that the particle gyrofrequency should be multiple of that for the K1600 cyclotron. Besides, the central field should be lower than 3 T as a spiral electrostatic inflector is used in the injection line. To provide a sufficient axial focusing of the beam, the sector spirality should be about 55° at extraction. A necessary room for placing the coil cryostat with super-isolation is ensured by having the distance between the superconducting coil and the valley shim and other parts of the magnet core no less than 70 mm. Also, the distance between the upper and lower parts of the coil should be about 170 mm to reliably withstand the acting ponderomotive forces on the coil fixation. The engineering current density in the coil is selected to be 70 A/mm².

The axial air gap between the sector surfaces is constant, being 52 mm with some enlargement in the central region. The gap value is selected to provide a necessary space between the sectors for installation of the electrostatic deflector for beam extraction. The required magnetic field dependence on the radius is obtained by decreasing the azimuthal span of the sectors from 50° in the center to 38° at the final radius. The field bump on the initial beam turns in the central region is produced by the central plug that has a central opening for the axial insertion of the spiral inflector. At the final radius the valley shims in the radial range of 20 mm decrease the valley gap from 540 mm to 244 mm. This configuration of the magnetic structure permits increasing the mean field at the edge of the magnetic system.

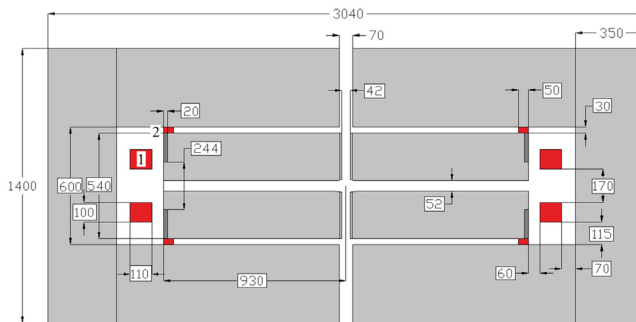


Fig. 5. Magnet cross section: 1 — main coil, 2 — correction coil.

Simultaneously, a necessary space for deployment of the acceleration system is provided.

Since the charge-to-mass ratio for H₂⁺ is larger by ~0.7% than for carbon, a slight increase of the magnetic field level or RF frequency is required to provide stable longitudinal motion of the beam. Since the RF frequency change by ~400 kHz would be too difficult to provide within the RF system design considered, the main coil current is proposed to increase by ~1%. This unfortunately leads to a rather large modification of the field index with a corresponding violation of the field isochronicity. It is shown that introduction of an additional trim coil in the magnetic system (Fig. 5) can return the field to the required isochronous one. The original magnetic field perfectly corresponds to the carbon acceleration (Fig. 6). Number of turns to reach the final energy ~270 for carbon and ~285 for H₂⁺ beams. The trim coil described above can be placed between the pole and the yoke, and its current density of ~6 A/mm² leads to a normal conducting design with 0.9 kA×turns per pole to ensure an acceptable phase slip for H₂⁺ beam. In this case, the main coil current should be increased by only 0.9%, considering an additional contribution from the trim coil to the field level.

The magnetic field levels in the iron return yoke and in the pole caps are at saturation. In particular, the field level in the yoke is about 2.4–2.5 T and in the pole is about 2.4–2.6 T. Concerning the iron production procedure, the special measures to ensure the required field quality has not yet been considered at this initial stage of the design.

In the magnetic field map the particle betatron frequencies are calculated by the SNOP code. The operation diagram (Fig. 7) shows that there are no crossings dangerous resonances in the acceleration range except the very last turns (2Q_z = 1), and the crossing of coupling resonances of the third and fourth order (2Q_r + 2Q_z = 3, Q_r - 2Q_z = 0, 2Q_r - 2Q_z = 1) takes place. The latter should be investigated in future beam dynamics modeling, but from general consideration no negative impact on the beam quality can be expected from them. Successful operation of similar cyclotrons with crossing of these resonances [13] confirms the above statement. In the selected magnetic structure the betatron frequency crosses the resonance Q_r = 1 (Fig. 7) in the last turns, which allows application of the precessional method for the beam extraction from the cyclotron.

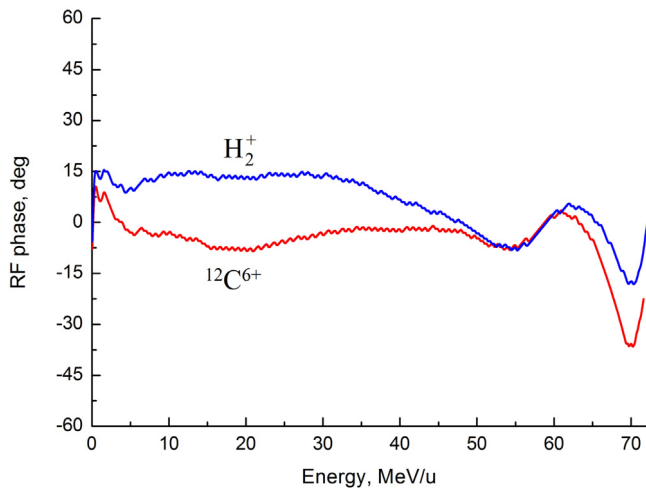


Fig. 6. RF phase evolution with particle energy during acceleration for both types of accelerated ions. The magnetic field is shaped for acceleration of carbon ions. The phase slip for H_2^+ ions is shown for the structure that uses the correction coil and increased main coil current by 0.9%.

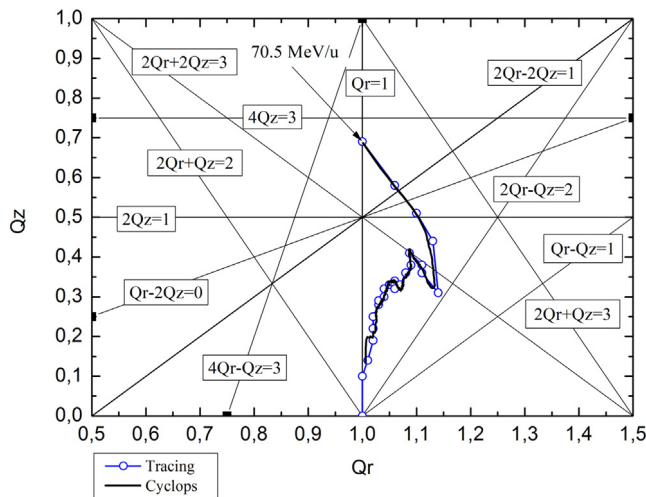


Fig. 7. Tune diagram. Betatron frequencies were calculated with the Cyclops code [14] and obtained by tracing.

Two sets of iron rods moving axially through the central line of the sectors are provided for the fine trimming of the magnetic field in the central region and at extraction. At the radius of 16 cm there are 3 rods (one rod for each sector) intended for the beam centering. For example, a careful design of the central region structure ensures that the amplitude of the radial betatron oscillation of the reference particle is less than 2 mm, which is quite satisfactory there. Also, applying additional 1st magnetic harmonic with the amplitude of 25 Gs generated by central iron rods permits decreasing the radial amplitude even more, namely, to 0.5 mm. The central iron rods can also be used for the beam correction in the case of magnetic field distortions due to, for example, an error in the main coil off-centering. In addition, 3 iron rods near the final radius (one per sector) can be used for the experimental optimization of the beam extraction efficiency.

4. Central region

The central region structure was carefully optimized to provide the best axial focusing and beam centering during acceleration in the cyclotron. The spiral inflector design with its RF shielding allows

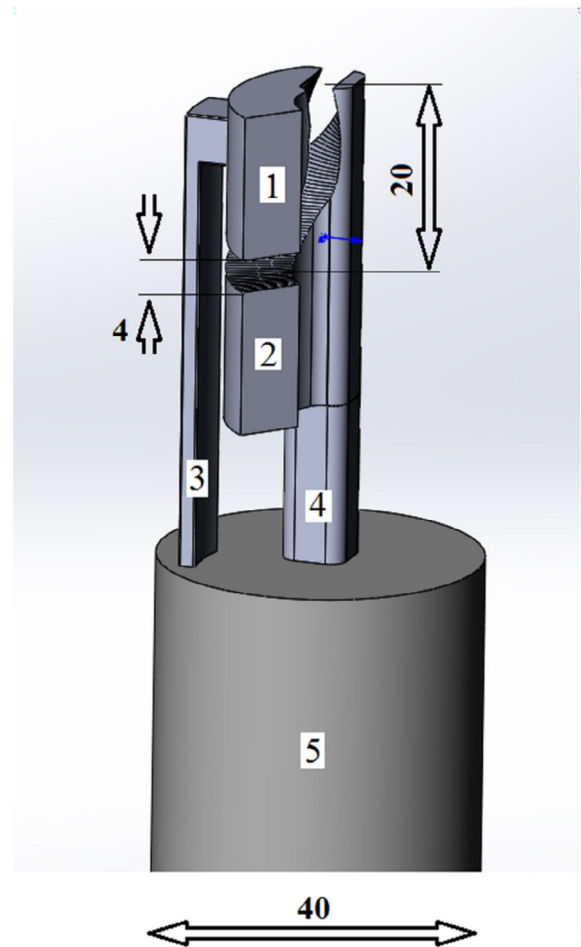


Fig. 8. Spiral inflector: 1 — negatively charged electrode, 2 — positively charged electrode, 3, 4 — potential leads providing fixation of the electrodes as needed, 5 — rod for insertion of the inflector to its working position.

sufficient space for the inflector potential leads (Fig. 8). In compliance with the transverse size of the beam the inflector aperture was chosen to be 4 mm. The electrical radius of the inflector is 20 mm for the potential of ± 6 kV on the inflector electrodes. The magnetic radius of the inflector is 13.4 mm. The inflector itself moves into the cyclotron axially to its working position inside the RF shielding attached to the dummy dees. There is a possibility of rotating the inflector inside the RF shield by several degrees for better matching of the injected beam to the central region acceptance. Also, the RF shield itself can rotate around its axis. Kilpatrick’s criterion was used to determine the acceleration gaps in the central region [15].

In the central region there are several posts attached to the dees and dummy-dees to provide sufficient scraping the so-called “tails” from the injected beam distribution over its cross section and, simultaneously, to increase the rigidity of the unit structure (Fig. 9). The axial aperture available for the beam passage is 6 mm on initial turns.

The beam dynamics analysis shows that the use of the buncher in the axial injection line would increase the beam transmission efficiency through the central region from 15% to 44% for both types of accelerated ions, carbon and H_2^+ . The majority of the particles get lost axially in the RF shield and in the puller, and $\sim 16\%$ of the beam is lost radially on the posts and $\sim 10\%$ inside the inflector.

5. Accelerating system

The cyclotron RF system consists of three cavities operating at 60.77 MHz with the third harmonic of the particle gyro frequency. As the

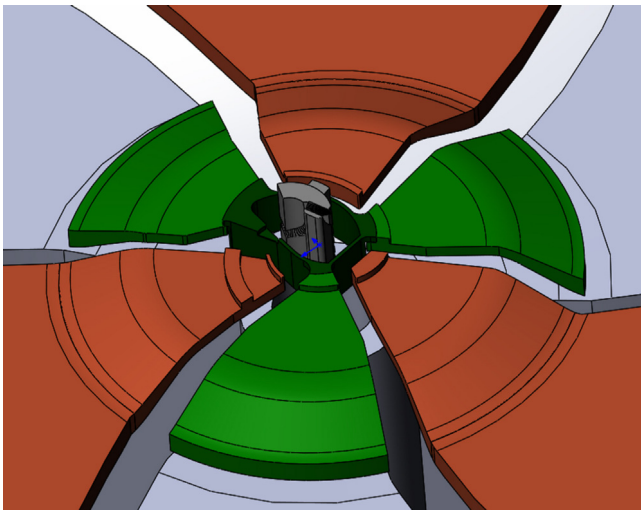


Fig. 9. Central region configuration.

central region is optimized for the best beam parameters necessary for the hadron therapy purposes, the resulting structure has three dees independent of one another. This leads to a requirement of three independent RF power lines and a separate excitation of each cavity. The voltage along the dees has to be profiled to achieve increased accelerating voltage at the higher radius leading to higher extraction efficiency. The dee axial aperture for the beam is 50 mm in the main acceleration zone.

The cavities have to be carefully designed with consideration of the Q factor, total power losses, and mechanical stability. The final technical design of the RF system is still an object of optimization and simulations in the CST Microwave Studio [16].

6. Extraction system

The extraction system is rather simple, and the extraction process can be easily carried out despite of the fact that all the valleys of the magnetic structure are occupied with the dees. The beam is extracted using the precessional extraction method driven by the 1st harmonic in the extraction region with amplitude of 3–5 Gs. In the calculations, the maximal value of the 1st magnetic harmonic was at $\sim 45^\circ$ upstream the deflector to push the beam to the MC1 mouth. The amplitude and the phase of the harmonic will be adjusted by movable iron rods, mentioned in Section 3.

Carbon ions are extracted by an electrostatic deflector (ESD) placed in the axial gap between the magnetic sectors, and two passive magnetic channels (Fig. 10). The electrostatic deflector has the field strength of 110 kV/cm, radial aperture of 10 mm, and uniform septum thickness of 0.1 mm.

Downstream the ESD the 1st magnetic channel is installed in the axial gap between the sectors. The required field distribution inside the radial aperture of the channel (field drop -0.17 T, transverse gradient 23 T/m) is obtained with the septum thickness of 5 mm and distance of ~ 18 mm between the last internal and deflected particle orbits. Unfortunately, the channel introduces some perturbation in the cyclotron magnetic field on the last internal orbits with the 1st magnetic harmonic as the main factor having a noticeable impact on the beam motion there. To reach sufficiently high beam extraction efficiency, this field perturbation should be suppressed as much as possible. The standard method for compensation of this field suggests placing of a dummy channel on the opposite side of the cyclotron. In our case it does not work since the corresponding space is already occupied by the dee. Another way of the channel field compensation implies insertion of iron pieces in the axial gaps of other two sectors, but one of these gaps

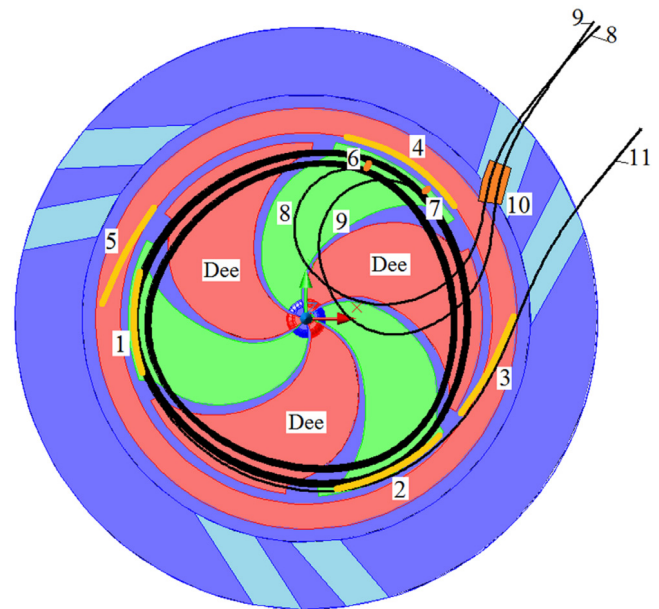


Fig. 10. Extraction system layout: 1 — electrostatic deflector, 2 — first magnetic channel, 3 — second magnetic channel, 4 — compensator of the first magnetic channel, 5 — compensator of the second magnetic channel, 6 — stripping foil location for extraction of 60 MeV protons, 7 — stripping foil location for extraction of 70 MeV protons, 8 — trajectory of 60 MeV protons, 9 — trajectory of 70 MeV protons, 10 — bending magnet for steering proton beams with output energy in the range (60–70) MeV, 11 — trajectory of 70 MeV/u $^{12}\text{C}^{6+}$ and H_2^+ beams.

is occupied by the electrostatic deflector. An alternative solution would be effective compensation of the perturbations at least in some selected radial range by a small modification of the sector geometry. In addition, a design of the channel with a minimal perturbation of the main magnetic field near the final radius can help even more. To this end, a set of shims shown in Fig. 11 can be used. Apparently, the radial range of this shimming can differ from that in the method described before. In the latter case, the adjustment of the channel position without noticeable impact on the beam motion becomes possible.

Concerning the 2nd magnetic channel (field drop -0.23 T, transverse gradient 25 T/m), it stays sufficiently far away from the internal beam orbits (~ 120 mm), leading to relatively small field perturbation there without noticeable influence on the beam motion. In addition, the dummy magnetic channel placed azimuthally opposite to the 2nd channel produces nearly complete compensation of its field despite of simpler structure compared to the channel itself.

Obviously, to achieve the most efficient beam extraction, the overall optimization of the extraction process by the corresponding adjustment of the extraction system parameters is required. Finally, it is also possible to slightly correct the magnetic field during its measurement campaign.

According our simulations the efficiency of the carbon beam extraction reaches $\sim 75\%$, and the output beam intensity is ~ 900 nA. Unfortunately, the transverse quality and the energy spread in the extracted beam are ~ 3 times worse than the desired ones for injection in the main K1600 cyclotron. Nevertheless, the required parameters of this beam can be reached in the beam preparation system of the MEBT (medium energy beam transport) line due to higher intensity (by ~ 4 times) compared to the requirement. For example, installation of a collimator with the aperture 5×4 mm² will result in beam intensity of 400 nA and emittances $\sim 3 \pi \cdot \text{mm} \cdot \text{mrad}$ (Table 2), which is quite sufficient for injection in the K1600. Given $\sim 70\%$ injection and $\sim 70\%$ extraction efficiencies expected in K1600, the final carbon beam after accelerator will be ~ 200 nA. After using energy selection system and beam spot cutting the beam intensity at the nozzle will be in several times smaller, but it is more than enough for hadron therapy.



Fig. 11. Configuration of the 1st magnetic channel and its field contribution: 1 — circulating beam, 2 — extracted beam.

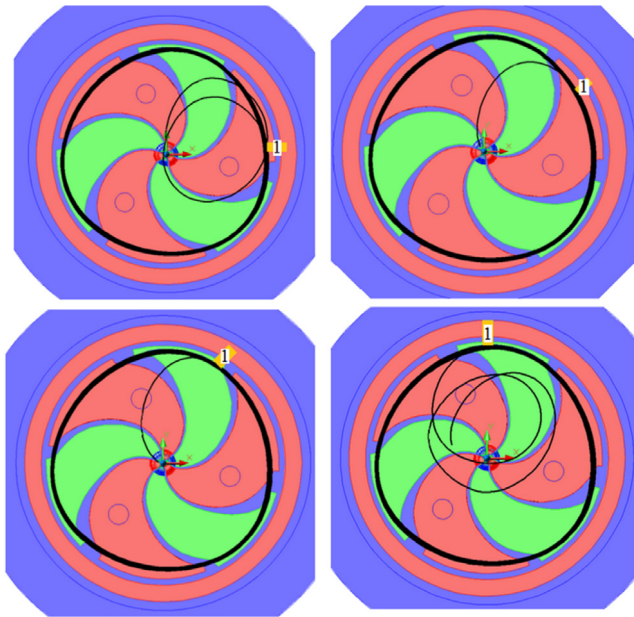


Fig. 12. Proton beam extraction by stripping of H_2^+ ions for various foil positions, labeled (1), for the acceleration along the sector spiraling.

The high-efficiency extraction of the proton beam can be obtained by stripping the H_2^+ ion beam on the foil inside the vacuum chamber of the accelerator. The method permits varying the outside beam energy in a limited range. Calculations show that it is rather difficult or even impossible to find the operational position of the stripping foil for the direction of the accelerated particle trajectory coincident with the sector spiraling. In this case, for some position of the stripping foil the extracted trajectory even returns to the cyclotron center with corresponding losses of particles there (Fig. 12). More to it, even the particles that still can make round the central region structure will be partially lost axially along number of turns needed to get back to the final radius resulting in very poor extraction efficiency in total. The effect takes place in the considered energy variation range of 60–72 MeV upstream the stripping foil.

The extraction efficiency is substantially higher for beam revolution opposite to the sector spiraling. In this case particles make only one turn after stripping before exiting the vacuum chamber (see Fig. 10). It should also be noted that the carbon extraction efficiency does not depend on the direction of acceleration. Calculating the output beam energy variation by changing the stripping foil position shows a drastic difference in the trajectories corresponding to various energies with no point in the cyclotron magnet yoke where these tracks belonging to different energies converge. For example, protons of relatively moderate energy of 35–40 MeV make two turns in the vacuum chamber, and their trajectories in the magnet yoke are fairly separated from the

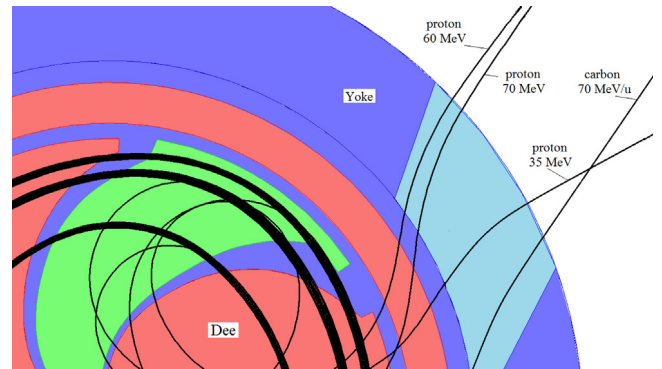


Fig. 13. Trajectories of the extracted beams.

corresponding paths of protons with higher energy, namely, 60–70 MeV (Fig. 13). Also, strong dependence of the beam axial envelope on the stripping foil position takes place. This effect limits the permissible energy variation of extracted protons above mentioned 60–70 MeV. Given output energy range very well matches the eye melanomas treating by the proton beam irradiation with additional decrease of the output energy (if needed) by the degrader in the beam transport line. Another way to extract protons with low energy by stripping H_2^+ ions would be direction of the proton beam to the opposite side of the cyclotron. Then, an additional beam transport line would be needed for direction of the extracted beam to a common interface point outside the machine. The line should have wide-aperture elements with the focusing property included.

3D simulation of the proton extraction by stripping H_2^+ ions shows that the axial size of the H_2^+ beam on the stripping foil reaches ~ 6 mm. The axial focusing of the proton beam downstream the stripping foil is not sufficient. As a result, the axial envelope of the proton beam increases drastically to 30–50 mm at the exit of the magnet yoke (Fig. 14), the main factor being the axial over-focusing near the main coil. Similar behavior of the extracted stripped beams found by measurements and/or calculations was reported for other cyclotrons [17,18]. The improvement can come from installation of a combined-function-dipole in the yoke outlet window. In addition to the increased axial focusing, the dipole can provide converging of 60–70 MeV proton paths in a common switching magnet in order to be transported through a single versatile set of beam lines. Calculations show that the extraction efficiency by the stripping reaches $\sim 95\%$ in this case. Given the ion source H_2^+ ions intensity of 1 mA and accelerated particle current of 440 μA upstream the stripping foil, the output proton beam intensity can reach $\sim 800 \mu A$.

It should be noted that high efficiency of the proton extraction by stripping is unavoidably accompanied by rather poor transverse beam quality (emittances of $30 \pi \cdot \text{mm} \cdot \text{mrad}$) outside the cyclotron. In addition, the energy spread in the output beam will be somewhat increased by the interaction of the particles with the stripping foil

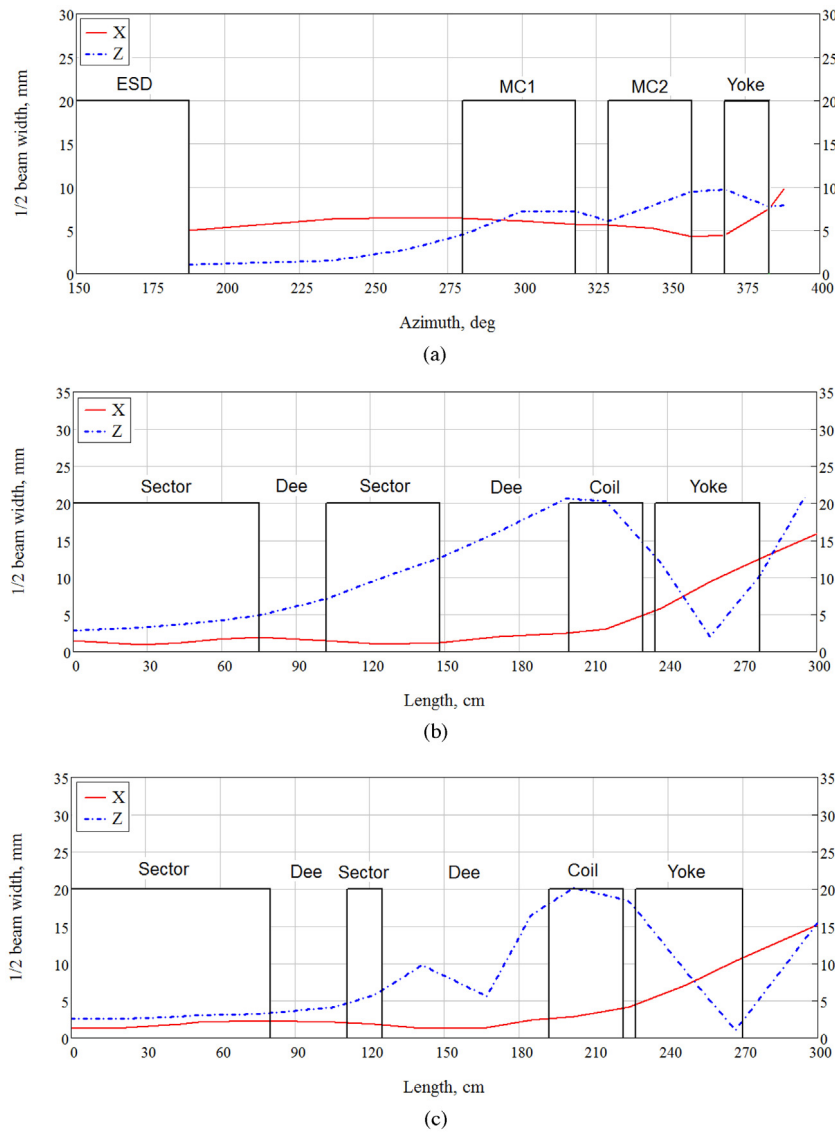


Fig. 14. Beam envelopes at extraction for 70 MeV/u carbon and H_2^+ ions (a), 70 MeV protons (b), and 60 MeV protons (c).

material. The problem could be solved by direct extraction of the H_2^+ beam using the same system as for carbon ions. Then, protons can be produced by stripping in the beam line outside the accelerator. The extraction efficiency in this case is $\sim 65\%$, and the output beam intensity of H_2^+ ions can reach $\sim 300 \mu\text{A}$. The resulting proton beam after stripping of H_2^+ ions can be $\sim 600 \mu\text{A}$ (Table 2). But it should be noted that the actual intensity of the output H_2^+ beam is strongly dependent on admissible heating of the ESD septum due to particle losses for a given extraction efficiency [19]. The effect requires additional investigation for the given machine parameters.

7. Beam delivery system

The layout of the beam lines for delivery of accelerated particles from the K280 cyclotron to the final user locations is given in Fig. 1. The design of the lines was performed by the Trace3D code. Parameters of the beam used for simulations were taken directly after 3D calculations of the beam dynamics through the cyclotron (see Table 2). The initial part of the beam delivery system consists of two beam lines (Fig. 15). One of the lines delivers the carbon beam for injection in the main K1600 machine and H_2^+ ions for stripping generation of the proton beam for isotope production. The other line is used to transport extracted protons for medical application as explained in the introduction.

Since the transverse focusing of the proton beam exiting the cyclotron is not enough, a few quadrupoles should be introduced to squeeze the beam envelope down to below 15 mm in the transport line. To this end, two types of quadrupoles with effective lengths of 300 mm and 200 mm and field gradients below $\sim 16 \text{ T/m}$ are used. In addition, the proton line has two 15-degree bending magnets of different radii. A quadrupole triplet ensures achromatic property of the line, which permits successful delivery of the beam to the treatment room even if the particle energy slightly deviates from the intended one. The length of these lines is about 5.5 m. The main design goal was to provide a beam spot of 2–3 mm at their final points where the energy selection system and collimators are located.

The requirement for a facility dedicated for eye tumour therapy is the provision of a proton beam with energy of 60–70 MeV and the energy spread less than 0.4% that are controlled by the energy selection system and horizontal slits. The final beam spot must be about 4 mm, ensured by a quadrupole before the nozzle of the eye setup. Envelopes of the proton beam from the energy selection system to the room for eye melanoma treatment are shown in Fig. 16. The beam transversal size at full length of the line of $\sim 20 \text{ m}$ is less than 15 mm. An achromatic line with quadrupole doublets and a triplet is used for bending the protons from the main transport line to eye treatment room. All of the

Table 2
Cyclotron beam characteristics.

Ion: acc./ extr.	Ion source output intensity μA	Extraction method	Central region transmission %	Collimator downstream the magnet yoke	Extraction efficiency %	Output beam Intensity μA	Output beam emittances hor./axial. $\pi \cdot \text{mm} \cdot \text{mrad}$	Output beam energy spread, %
$^{12}\text{C}^{6+}$	3	ESD		NO	73	0.9	23/22	± 0.26
$^{12}\text{C}^{6+}$	3	ESD	44	YES	33	0.4	3/2	± 0.16
H_2^+/p	1000	Stripping		NO	95	800	30/20	± 0.67
H_2^+	1000	ESD		NO	65	300	21/20	± 0.28

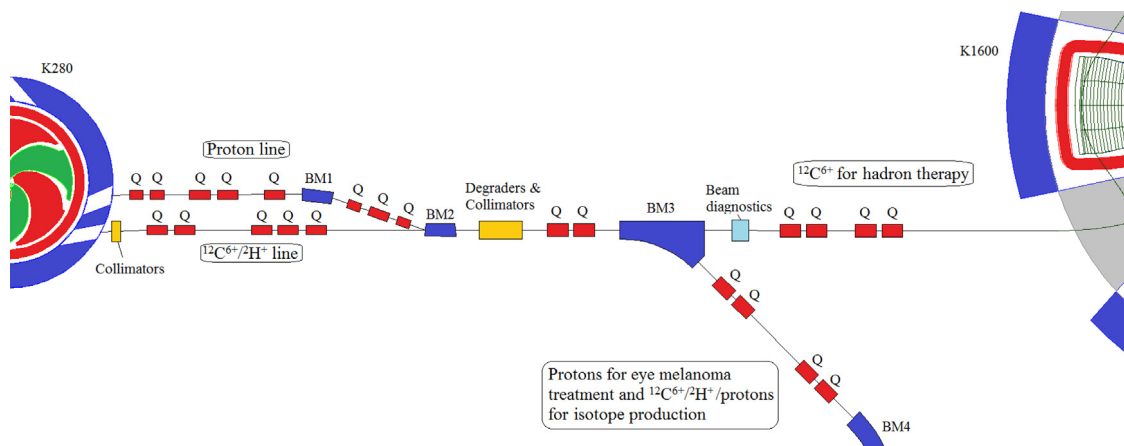


Fig. 15. Selected part of the beam delivery system. The energy selection system begins from the bending magnet BM1 and ends at the bending magnet BM3.

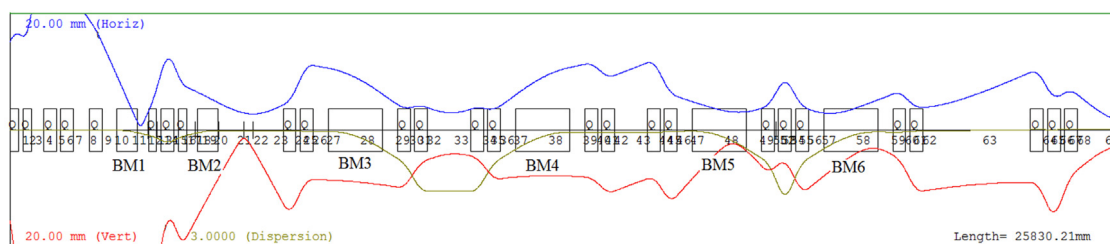


Fig. 16. Proton beam envelopes in the transport line from the cyclotron exit to the eye melanoma treatment room.

quadrupoles after the extraction line are with the same effective length of 300 mm and maximal gradient of 14 T/m. The line has a lot of free space for installation of other beam controlling and diagnostics systems.

The same principles as described above (achromatic property, beam envelopes under 15 mm, and final beam spot about 3 mm) are used for development of a transport line for delivery carbon and H_2^+ ions to the room for isotope production. The length of this line is ~ 30 m.

Since the K280 cyclotron is used for injection of the carbon beam to the K1600 cyclotron, one more line was designed to transport the carbon ions between two cyclotrons. The length of this line is ~ 13 m, and the field gradient of the quadrupoles is not more than 16 T/m.

8. Summary

The calculations conducted in compliance with the development of the cyclotron complex for hadron therapy show that the construction of the injector-cyclotron K280 can be practically realized. All systems of the cyclotron can be based on the existing designs and technologies. The accelerator generates beams of carbon and H_2^+ ions with the beam output energy of 70 MeV/u and intensities of 0.9 μA and 300 μA , respectively. The latter estimation should be additionally confirmed by taking into account its strong dependence on admissible heating of the ESD septum during extraction. The output proton beam intensity of 800 μA can be obtained by stripping H_2^+ ions inside the cyclotron. In addition to the main purpose of the machine as an injector of the carbon beam to the K1600 cyclotron, the accelerator can also be used

as a stand-alone facility for medical applications: treatment of eye melanomas and skin cancer and isotope production. Other ions (alpha-particles, for example) with charge-to-mass ratio of 0.5 can also be accelerated in the machine without any problem. With the weight of 70 t and size of 3 m, the cyclotron has many apparent advantages over other room-temperature or superconducting machines of similar destination but with the charge-to-mass ratio of 1. The former normally accelerate H^- ions with the possibility of varying the output energy of the beam but have rather large weight and footprint. The latter with a high magnetic field are not able to accelerate H^- ions due to massive particle losses by electromagnetic stripping, and there is the only possibility to using direct acceleration of protons instead. Then, the electrostatic deflector should be used for particles extraction, which leads to decreasing extraction efficiency and problems with the beam energy variation.

Finally, the staging approach to the cyclotron complex for hadron therapy allows practical application of the 1st cascade (K280) immediately after the machine commission.

References

- [1] V.L. Smirnov, S.B. Vorozhtsov, Feasibility study of a cyclotron complex for hadron therapy, *Nucl. Instrum. Methods Phys. Res. A* 887 (2018) 114–121.
- [2] J.M. Schippers, et al., A novel design of a cyclotron based accelerator system for multi-ions therapy, in: Proc. of the Int. Conf. on Heavy Ion Accelerator Technology, HIAT'09, Venice, Italy, 2009, pp. 74–78.

- [3] A. Denker, C. Rethfeldt, J. Röhrich, D. Cordini, J. Heufelder, R. Stark, A. Weber, Advocacy for a dedicated 70 MeV proton therapy facility, in: Proc. of CYCLOTRONS 2010, Lanzhou, China.
- [4] M.T. Christóvão, T.P. Ribeiro de Campos, B.M. Trindade, Simulation and dosimetric analysis of proton and carbon ion therapy in the treatment of uveal melanoma, *Radiol Bras* 44 (6) (2011) São Paulo Nov./Dec..
- [5] L. Calabretta, et al., LNS Catania project for therapy and radioisotope production, in: Proc. of CYCLOTRONS'04, 18–22 Oct 2004. Tokyo, Japan, pp. 72–76.
- [6] V.L. Smirnov, Computer modeling of a compact isochronous cyclotron, *Phys. Part. Nucl.* 46 (6) (2015) 940–955.
- [7] Y. Iwata, et al., Present status of a superconducting rotating-gantry for carbon therapy, in: Proc. of HIAT2015, Yokohama, Japan, 2015.
- [8] <http://www.pantechnik.com/#!/sources/vstc2=supernanogan>.
- [9] C. Bieth, S. Kantas, P. Sortais, D. Kanjilal, G. Rodrigues, Recent development in ECR sources, *Nukleonika* 48 (Supplement 2) (2003) S93–S98.
- [10] <http://laacg.lanl.gov/laacg/services/services.phtml>.
- [11] V.L. Smirnov, S.B. Vorozhtsov, SNOP – beam dynamics analysis code for compact cyclotrons, in: Proc. of the XXIII Russian Accelerator Conference, RuPAC'2012, St. Petersburg, Russia, 2012, pp. 325–327.
- [12] V.L. Smirnov, Computer codes for beam dynamics analysis of cyclotronlike accelerators, *Phys. Rev. Accel. Beams* 20 (2017) 124801.
- [13] J.M. Schippers, D.C. George, V. Vrankovic, Results of 3D beam dynamic studies in distorted fields of a 250 MeV superconducting cyclotron, in: Proc. of CYCLOTRONS'04, 18–22 Oct 2004. Tokyo, Japan, pp. 435–437.
- [14] M.M. Gordon, Computation of closed orbits and basic focusing properties for sector-focused cyclotrons and the design of “CYCLOPS”, *Part. Accel.* 16 (1984) 39.
- [15] Silvia Verdú Andrés, Literature research on Kilpatrick's criterion, CLIC Experimental & Breakdown Studies Meeting, CERN, 2009.
- [16] CST Microwave Studio software, Computer Simulation Technology Co.
- [17] G.G. Gulbekyan, O.N. Borisov, V.I. Kazacha, Extraction by stripping of heavy ion beams from cyclotrons, in: Proc. of HIAT'09, Venezia, Italy, 2009.
- [18] L. Jasna, Ristic'-Djurovic, Stripping extraction of positive ions from a cyclotron, *Phys. Rev. Accel. Beams* 4 (2001) 123501.
- [19] D. Vandeplassche, et al., Extraction Simulations for the IBA C70 Cyclotron, in: Proc. of the Cyclotrons and Their Applications 2007, Eighteenth International Conference, pp. 63–65.